RSC Advances

ROYAL SOCIETY OF CHEMISTRY

www.rsc.org/advances

RSC Advances

RSCPublishing

ARTICLE

Label-free cell phenotypic profiling identifies pharmacologically active compounds in two Traditional Chinese Medicinal plants

Cite this: DOI: 10.1039/x0xx00000x

Received 00th April 2014,
Accepted 00th April 2014

DOI: 10.1039/x0xx00000x

www.rsc.org/

Xiuli Zhang[a,‡], Huayun Deng[b,‡], Yuansheng Xiao[a], Xingya Xue[a], Ann M. Ferrie[b], Elizabeth Tran[b], Xinmiao Liang[a,*], and Ye Fang[b,*]

Traditional Chinese Medicines (TCMs) are widely used in clinical practice and natural products have been a rich resource for drug discovery. Identification of pharmacologically active chemical constituents is essential to the future of TCMs and natural product-based drug discovery. Here we report a label-free cell phenotypic profiling strategy to identify active fractions and compounds of two TCM plants including *Paederia scandens* (*Lour.*) *Merri.* (Jishiteng in Chinese) and *Millettia pachyloba* Drake (Duyuteng in Chinese), and to determine their mechanisms of action. The extracts of both plants were first fractionated to 160 fractions. Label-free cell phenotypic profiling afforded by resonant waveguide grating biosensor in microplate were then used to identify the active fractions acting at three different cell lines including A431, A549 and HT29. Mass spectroscopy-directed purification was then used to identify and purify active compounds. NMR and mass spectroscopy were used to determine the chemical structures of the active compounds, and pharmacological assays were used to elucidate their mechanisms of action. Using this strategy, we have discovered that both medicinal plants contain moderately high amount of niacin, an agonist for hydroxyl carboxylic acid receptor-2. Literature mining further suggests that the presence of niacin in *Paederia scandens* may be responsible for its antidyslipidemic effect found in clinic studies. This study demonstrates the potential of label-free cell phenotypic profiling for identifying active fractions and compounds of TCMs as well as elucidating their mechanisms of action.

Introduction

Traditional Chinese Medicines (TCMs) including various forms of herbal medicine and dietary therapy have been in clinical practice since several thousands of years ago. Essential to the modernization of TCMs is to identify pharmacologically active chemical constituents and their mechanisms of action.[1-3] For instance, the *Compound Danshen Dripping Pill* contains active fractions of *Danshen*, the dried root of *Salvia miltiorrhiza*, and is currently in Phase III trial for the treatment of cardiovascular and cerebrovascular diseases with a high hope to become the first US Food and Drug Administration approved TCM.[4,5]

Natural products have been proven to be a rich source for drug discovery.[6-15] Natural products (secondary metabolites) and their derivatives account for a great portion of molecular medicines, although there has been a decline in the past fifteen years, in part due to the shift to high-throughput screening of synthetic libraries.[15] Given the untapped biological resources[16] and the adoption of new technologies including synthetic biology[17] and phenotypic assays[18], natural product**s** still remains to be an attractive revenue for drug discovery.

In the recent years, label-free biosensors including resonant waveguide grating (RWG) biosensors in microplate have become an attractive alternative for drug profiling and screening.[19-21] The dynamic mass redistribution (DMR) signal arising from drug action in native cells, as recorded by RWG biosensors**,**[22] represents a cell phenotypic response, permitting mechanistic deconvolution of receptor biology[23-25] and drug pharmacology[26-28]. Here we report a label-free cell phenotypic profiling-centric strategy (**Fig.1**) to identify active chemical constituents from two TCM plants, *Paederia scandens (Lour.) Merri.* (Jishiteng in Chinese) and *Millettia pachyloba Drake* (Duyuteng in Chinese) and elucidate their mechanisms of action. *Paederia scandens* is a relatively widely studied TCM used to treat chest pain, inflammation of the spleen, and rheumatic arthritis,[29] while *Millettia pachyloba* is poorly studied. The leaf, stem and root of *Paederia scandens* are known to contain a variety of iridoid glucosides,[30,31] sterols, triterpenes, alkanes, fatty alcohols, fatty acids, phenylpropanoid including caffeic acid and coumaric acid,[32] and flavonoids including quercetin[33].

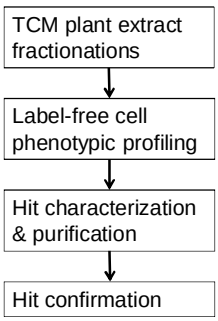

FIGURE 1. A label-free cell phenotypic profiling centric strategy for identifying active chemical constituents from TCM plants and elucidating their mechanisms of action.

Experimental

Materials

Acipimox, formic acid, niacin, nicotinyl alcohol, nicofuranose, and pertussis toxin (PTx) were purchased from Sigma Chemical Co. (St. Louis, MO, USA). The preparative grade acetonitrile and methanol was obtained from Fulltime (Anhui, China). PTx was lyophilized and stocked under dry condition at -20ºC, and diluted using the complete cell culture medium before use. All other compounds were stocked in dimethyl sulfoxide (DMSO) at 100 mM, and were diluted to the indicated concentrations using the assay buffer (1×Hank's balanced salt buffer, 20mM Hepes, pH 7.1; HBSS). Epic® 384-well cell culture compatible biosensor microplates were obtained from Corning Incorporated (Corning, NY, USA).

Cell culture

All cell lines, human colorectal adenocarcinoma HT29, human epidermoid carcinoma A431, and human alveolar basal epithelial adenocarcinoma A549, were obtained from American Type Cell Culture (Manassas, VA). All cell lines were cultured using corresponding medium supplemented with 10% fetal bovine serum, 4.5 g/L glucose, 2 mM glutamine, 100 µg/ml penicillin and streptomycin at 37°C with 5% CO_2. The medium used was McCoy's 5A medium modified for HT29 cells, Dulbecco's Modified Eagle's Medium for A431 cells and A549 cells. The native cells were passed with trypsin/EDTA (ethylenediaminetetraacetic acid) when approaching 90% confluence to provide new maintenance cultures on T-75 flasks and experimental cultures on the biosensor microplates or chambers. For cell culture in Epic® biosensor microplates, the optimal seeding densities were found to be 32 K, 25 K, and 20K per well for HT29, A431 and A549 cells, respectively. Previously, we had found that DMR profiles of several receptors in A431 are quite sensitive to cellular status and cells in quiescent state generally gave rise to more robust DMR than those in proliferating states.[21,23,26] Therefore, A431 cells were cultured in the complete medium overnight followed by overnight starvation in the serum free medium. On the other hand, both A549 and HT29 cells only cultured in the completed medium for 24hrs were found to be optimal. Afterwards, all cells were washed three times using a plate washer (Bio-Tek Microplate Washers ELx405t, Bio-Tek, Winooski, VT) and incubated in the HBSS buffer for about one hour before DMR assays. The confluency for all cells at the time of assays was ~95%.

Extraction and fractionation of TCM plants

The TCM *Paederia scandens* whole plants and *Millettia pachyloba* stems, the identity of which were confirmed by Xiaoping Yang, were purchased from Suizhou (Hubei, China) and used for extraction. The extraction procedure used was identical for both TCM plants. Specifically, the plants of 5 kg were pulverized and refluxed with 50 kg water for 1 hr. The high amount of TCM plants used was to establish our extraction and fraction libraries for screening and follow-up confirmation studies. The reflux was then filtered and the residue was refluxed again with 50 kg water for 1 hour. After filtration, the two extract solutions were combined (about 100 L), and was then processed with a 70000 molecule-sized hollow fiber membrane. After filtration, the solution obtained was condensed under vacuum at 60 ºC to 1050 ml. Fractionation was performed using mass-directed purification system (Waters, Milford, MA, USA) which consists of a binary BMG2525 pump, a 2777 autosampler, a ZQ mass spectrometry, a 2487 UV detector, a 2757 sampler manager and a Sunfire® 50 x 150mm, 5µm column. For each fractionation, the loading volume of the condensed extraction solution was 140µl and 110µl for *Paederia scandens* and *Millettia pachyloba*, respectively. The amounts of fractions collected were found to be sufficient for the fraction screening. The mobile phase used was 0.1% (v/v) formic acid in water (phase A), and methanol and acetonitrile with a ratio of 20 to 80 (v/v) (phase B). The separation linear gradient (formatted as "time (v%, B concentration)") was 0 min (10%, B) - 30 min (80%, B) - 35 min (100%, B) – 60 min (100%, B). The flow rate was: 0 min (90 ml/min) – 30 min (90 ml/min) - 35 min (80 ml/min) – 60 min (80 ml/min). Both total ion and UV at 254nm were used for detection. The fraction collections were started at 2 min till 55.3 min, and three fractions were collected every minute. Total 160 fractions were collected for each plant extract. The fractions were then aliquoted and dried under vacuum. The dried fractions were then dissolved in DMSO to 2 mg/ml, and diluted using the assay buffer before profiling.

Secondary fractionation of active fractions

Once identified, the active fractions were then subject to secondary fractionation using e2695 Purification system the same as in first fractionation. The original fraction JST-003 was used to afford secondary fractions using the ClickIon 20×250mm, 10µm column (Acchrom, China). The flow rate was 20 ml/min. The mobile phase was 0.1% (v/v) formic acid in water (phase A) and 0.1% (v/v) formic acid in methanol (phase B). The linear gradient (formatted as "time (v%, B

concentration)") was 0 min (3%, B) – 15 min (25%, B) -20 min (95%, B). Based on mass spectrum and UV peaks, five secondary fractions were collected, named as JST-003-#1 to JST003-#5.

Purification of active compounds

To purify the active compounds, first dimension preparation was performed at preparative scale using hydrophilic interaction chromatography (HILIC) separation mode with the Click Ion 20×250mm, 10μm column (Acchrom, China). UV at 260 nm was used as the detector. The flow rate was 20 ml/min. The mobile phase was 0.1% (v%) formic acid in water (phase A), 0.1% (v%) formic acid in acetonitrile (phase B). The gradient (formatted as "time (v%, phase B concentration)") was 0 min (95%, B) – 10 min (82%, B) – 20 min (82%, B) – 35 min(40%, B). Afterwards, a second dimension orthogonal purification of fractions obtained using the first dimension preparation was carried out at Alliance HPLC with 2998 PDA detector (Waters). The column used was XAqua 4.6mm×250mm, 10μm with a flow rate of 1 ml/min. The isocratic separation was completed in reverse phase mode with 0.1% (v) formic acid in water as mobile phase lasting for 15 min. The purity of purified compounds were performed on Alliance e2695 with two columns under two LC conditions, the reverse phase analysis on column XAqua 4.6×250mm, 10μm, and the HILIC analysis on column ClickIon 4.6×250mm, 10μm. All conditions consisted of mobile phase A of 0.1% (v) formic acid in water and mobile phase B of 0.1% (v) formic acid in acetonitrile. The flow rate was 1 ml/min. The gradient of HILIC separations (formatted as "time (v%, phase B concentration)" was 0 min (95%, B) – 25 min (65%, B).

Nuclear magnetic resonance (NMR) and MS analysis of active compounds

NMR spectra were collected using Bruker AVIII 600 MHz NRM spectrometer equipped with software of TOPSIN 3.0, and samples dissolved in D_2O. MS spectra were obtained using Orbitrap Elite mass spectrometry under either positive mode or high duty cycle mode with 180 voltages (ThermoFisher Scientific, MA, USA).

Total niacin determination

To determine the total amount of niacin in both plants, 100g of the herb plant was grinded to powder. 1g powder was then suspended in 10 ml water in a 250 ml round bottom flask with a reflux condenser. After 2 hrs reflux the supernatant was collected, and the remaining residue was refluxed again. Both supernatants were then combined and concentrated down to 10 ml. 5 ml of the concentrated solution was frozen dried in -45^{o}C using a lyophilizer and weighed. Another 5ml of the concentrated solution was used to quantify niacin using a HPLC system consisting of an ACCELA 1250 Pump and an ACCELA Autosampler (Thermo Scientific). Chromatographic separation was carried out on a Click-Ion (250 mm×4.6 mm I.D., 5 μm; Accrom, Beijing) column maintained at ambient temperature (21^{o}C). The mobile phase A was 0.1% (v) formic acid in water, and the mobile phase B was 0.1% (v) formic acid in acetonitrile. The flow rate was 1 ml/min. The gradient started at 5% mobile phase A, and linearly reached to 10% in 15 min, then arrived to 60% in 5 min, and last kept at 60% for another 10 min. The flow rate is 1.0 ml/min. The injection volume was 5 μL. MS detection was performed on a Thermo TSQ Quantum Ultra triple quadrupole mass spectrometer (Thermo Scientific) equipped with an ESI source in the positive ionization mode. The MS operating conditions were optimized as follows: the spray voltage was 3000 V, the vaporizer temperature was 500 ^{o}C, the capillary temperature was 400 ^{o}C, the sheath gas (nitrogen) pressure was set to 75, the auxiliary gas (nitrogen) pressure was set to 20, the collision gas (argon) pressure was 1.5 mTorr. Quantification was obtained using the MRM mode with a scan time of 0.25 sec per transition. Standard solutions of niacin from 0.01 to 100 μg/ml were prepared in water.

DMR assays in microplate

DMR assays in microplate were carried out using conventional Epic® system (Corning), a standalone and high throughput screening compatible label-free wavelength interrogation reader system tailored for RWG biosensors in microplates.[34,35] For DMR assays in microplate, the cells were washed three times with the HBSS and further incubated with the buffer for 1 hr inside the reader system. Afterwards, a 2-min baseline was first established and normalized to zero. The DMR signals of compounds were then recorded as the shift in the resonant wavelength (picometer, pm) as a function of time, after the compound solutions were transferred into the biosensor wells using the on-board liquid handling device. For toxin treatment, cells were pretreated with 100 ng/ml PTx for overnight in the complete medium at 37 °C/5% CO_2, followed by washing twice with HBSS and 1 hr incubation insider the reader. All studies were carried out with at least three replicates, unless specifically mentioned.

Quantitative real-time PCR (qRT-PCR)

Total RNA was extracted from cells using an RNeasy mini kit (Qiagen, Cat#74104). On-column DNase digestion was performed using RNase-free DNase set (Qiagen, Cat#79254) to eliminate genomic DNA contamination. The concentration and quality of total RNA were determined using a Nanodrop 8000 (Thermo Scientific). Customized PCR-array plates for 352 GPCR genes and reagents were ordered from SABiosciences (Qiagen, Valencia, CA). About 1 μg total RNA was used for each 96-well PCR-array. The PCR-array was performed on an ABI 7300 Real-Time PCR System following the manufacturer's instructions.

Whole cell cyclic AMP (cAMP) assays

Inhibition of the forskolin-stimulated cAMP accumulation in A431 cells was performed using the cAMP-Glo assay kit (Promega, Madi-son, WI), according to the manufacturer's

instructions (Promega, Cat#V1502). Briefly, cells were plated in 384well tissue culture treated plates (Corning) with a seeding density of 20000 cells per well. Cells were cultured in the serum rich medium overnight. Next day, the media was removed, and cells were incubated with compounds in the presence of 5 µM forskolin in cAMP induction buffer for 30 minutes. The reaction was terminated by adding lysis buffer and luminescence was measured using Tecan Safire II reader.

Data visualization and clustering

For each DMR the responses at the six distinct time points (3, 5, 9, 15, 30, and 45min post stimulation) were extracted for similarity analysis. All time points refer to the stimulation duration after renormalized the responses starting from the time when the compound was added. For visualization purpose the responses were colour coded to illustrate relative differences in DMR signal amplitude (red: positive; green: negative; black: zero). In the ligand-DMR matrix each column represents a DMR response at a particular time in a specific assay condition, and each row represents one ligand (**Fig.2**). Every row and column carries equal weight. The Ward hierarchical clustering algorithm and Euclidean distance metrics (http://www.eisenlab.org/eisen/) were used for clustering the TCM fractions.[26,36,37] DMSO in the vehicle at a concentration that equals to those for all fractions was also included as a negative control. Each fraction was assayed at four replicates. The averages of the four replicates were used for analysis. All DMR signals were background corrected using the corresponding in-plate negative controls.

Statistical analysis

DMR dose response data were analysed by using GraphPad Prism 5.0 (GraphPad Software Inc., San Diego, CA, USA). The EC_{50} or IC_{50} values were obtained by fitting the dose DMR response curves with nonlinear regression. For the liquid chromatography–mass spectrometry (LC-MS) analysis, Masslynx 4.1 (Waters) software was used.

Results and discussion

Fractionation of TCM plant extracts

Two TCM plants, *Paederia scandens* whole plants (JST) and *Millettia pachyloba* stems (DYT), were chosen for the present study. The extracts generated from these two plants were fractionated to 160 fractions, named JST-001 to JST-160, or DYT-001 to DYT-160, respectively. Given the relatively low resolution of the fractionation protocol used to separate compounds and the medicinal plants contain many different classes of compounds, it is expected that a specific fraction may contain multiple compounds, and one specific compound may present in multiple consecutive fractions but at different concentrations.

Label-free cell phenotypic profiling of TCM plant fractions

Given the wide pathway coverage and high sensitivity,[19-24] the label-free cell phenotypic assay afforded by RWG biosensor was used to profile all 320 fractions against three cancerous cell lines, A431, A549 and HT29. Each fraction was assayed at 2 µg/ml with four replicates across the three cell lines, in order to minimize some undesirable responses or adverse effects on desirable responses caused by the impurities in the fractions. The DMR arising from the stimulation of a specific cell line with each fraction was obtained individually and used to determine its agonist activity in the cell line. The averaged DMR signal of each fraction in an assay was then translated to a six-dimensional coordinate (that is, the real DMR responses at six distinct time points including 3, 5, 9, 15, 30 and 45min post stimulation) for effective similarity analysis, which, in turn, may be informative about their underlined biological activity. We found that the six time points are adequate to capture the main characteristics of all DMR in all the three cell lines. For each cell line the negative control (that is, the assay buffer containing equal amount of DMSO) was included to define the range of responses for classification of the agonist activity of these fractions. Fractions whose DMR were smaller than 60 pm and similar to the negative controls across all cell lines were considered to have no agonist activity and excluded from similarity analysis, except for these that clearly blocked the DMR arising from subsequent stimulation with YE210, a known GPR35 agonist, in HT-29 cells (see below). Similarity analysis using unsupervised Ward hierarchical clustering algorithm and Euclidean distance metrics led to a label-free cell phenotypic heat map, which categorized these fractions into four major clusters (**Fig.2**).

Several interesting features emerged. First, the plant *Paederia scandens* extract contains less active fractions than the *Millettia pachyloba* extract. Among 69 active fractions, only twelve are from the *Paederia scandens* extract.

Second, the hit rate was relatively high. Out of the 320 fractions in total, fifty-four directly triggered a detectable DMR with an amplitude greater than 60pm in at least one of the three cell lines. This high hit rate was in part due to the complexity in active constituents in TCM plant extracts, in part due to the fact that DMR agonist assay have high target/pathway coverage and high sensitivity, and also due to the crude fractionation approach used which may cause an abundant compound to be collected unevenly in multiple consecutive fractions.

Third, most of the fifty-four fractions that displayed agonist activity in at least one cell line were found to be associated with discrete fraction groups, each of which consists of multiple consecutive fractions and shares similar label-free phenotypic profiles (**Supplementary Figs. 1 to 5**). We speculated that the smaller the group is the higher possibility is for a single active compound to be responsible for the observed label-free phenotypic activity of these fractions within the same group. For instance, the fraction group including JST-001 to 004 and DYT-001 to 005 was only active in A431, leading to a rapid and transit positive DMR. For both plant extracts, the third fraction, JST-003 or DYT-003, gave rise to the greatest response (**Fig.3**). Given the similarity in label-free cell

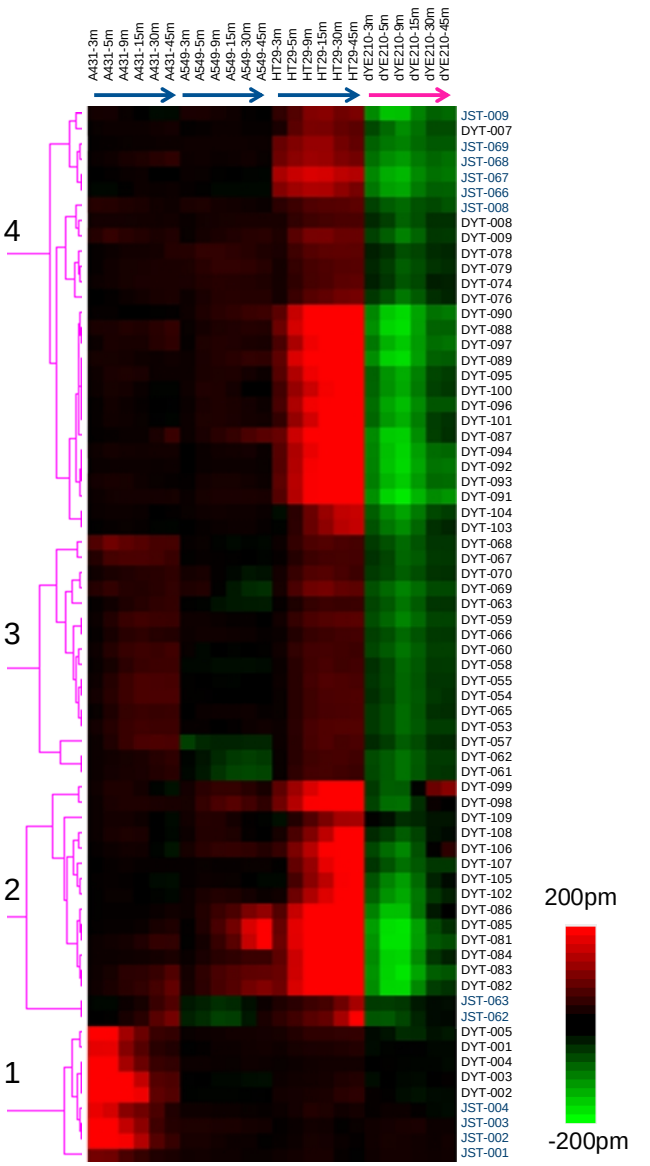

FIGURE 2. Label-free cell phenotypic heat map of two TCM plant fractions in three cell lines including A431, A549 and HT29. This heat map was obtained using similarity analysis of the DMR signals of the fractions in the three cell lines, and the net change of the DMR of the GPR35 agonist YE210 at 1 μM in HT29 induced by the pretreatment with a specific fraction. For each agonist profile, the real amplitudes at 3, 5, 9, 15, 30 and 45min post stimulation were used and colour coded – Green: negative; Red: positive; black: zero response. For the DMR of 1 μM YE210 in HT29, the net difference between the fraction-pretreated cells and the buffer-pretreated cells was used and also colour coded – Green: suppression; Red: potentiation; Black: no change. False colour scale bar is included to assist the data visualization.

phenotypic activity, the DMR of these fractions in A431 may be due to the activation of a single endogenous receptor induced by a single hydrophilic small molecule. Furthermore, the differences in signal amplitude may be due to the uneven distribution of the active molecule among these consecutive fractions in each plant, so the DMR of these fractions within a group could mimic the dose response. This was confirmed by follow-up studies (see below). On the other hand, the group DYT-081 to 109 is quite large, indicating that multiple compounds may be responsible for the DMR detected.

The activity of TCM plant fractions at GPR35

Many medicinal plants are rich in natural phenols,[38,39] several of which have been identified to be agonists for GPR35, a G protein-coupled receptor (GPCR). These GPR35-active natural phenols include luteolin and quercetin,[40] gallic acid and wedelolactone,[41] (+)-taxifolin,[42] baicalein, morin, myricetin, lapachol, lobaric acid, laccaic acid A, hematein, α-cyano-4-hydroxycinnamic acid, ellagic acid, and 7-deshydroxy-pyrogallin-4-carboxylic acid.[43] These natural phenols display a wide range of agonist activity at the GPR35 with nanomolar to low micromolar potency. Given that some of the agonistically active fractions including the group of DYT-081 to DYT-086 gave rise to a DMR signal similar to that arising from the activation of endogenous GPR35 in HT-29 (**Supplementary Figs. 1-4**), we speculated that some active fractions may contain GPR35 agonist(s).

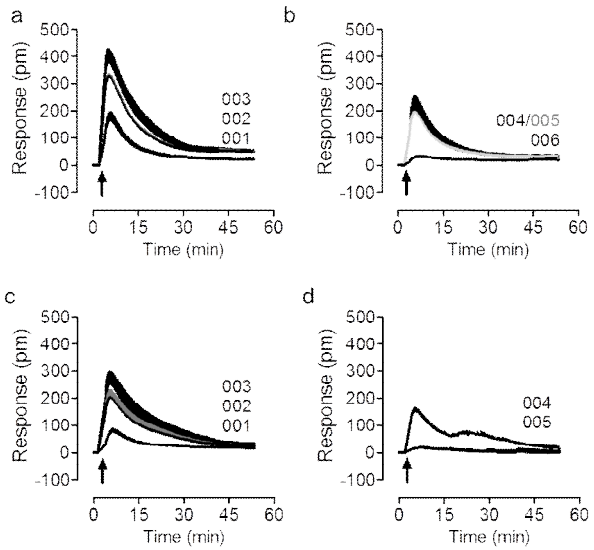

FIGURE 3. The real-time DMR of DYT-001 to 005 (a,b), or JST-001 to 005 (c,d) in A431 cells. The arrow indicates the time when the fraction was added. Data represents mean±s.d (n=4).

To test this, we applied two-step DMR desensitization assay[44] to examine the ability of all fractions to block or desensitize the DMR arising from sequential stimulation with YE210 in HT29. YE210 is a known putative GPR35 agonist and HT29 endogenously expresses GPR35.[45] To better illustrate the effects of these fractions to block or desensitize the YE210 DMR, we performed similarity analysis of the agonist activities of all fractions in the three cell lines, together with the net changes in the YE210 DMR after 1hr pretreatment with all fractions, each individually. Similarity analysis suggested that the sixty-nine active fractions were classified into four major clusters. The first cluster consists of nine fractions including JST-003 and DYT-003, all of which were active specifically in A431, and had little effect on the YE210 DMR in HT29, suggesting that these fractions do not contain GPR35 agonist.

The second cluster consists of sixteen fractions including JST-062 and DYT 085; most of these fractions exhibited noticeable agonist activity in all three cell lines, and markedly suppressed the YE210 DMR, suggesting that some of these fractions contain GPR35 agonists. The third cluster consists of sixteen fractions including DYT-055 and DYT-068; these fractions triggered small but noticeable DMR in both HT-29 and A431, and slightly suppressed the YE210 DMR, suggesting that these fractions contain no or little amounts of GPR35 agonists. The last cluster consists of twenty-eight fractions including JST-009 and DYT-090; most of these fractions exhibited agonist activity specifically in HT-29, and greatly suppressed the YE210 DMR when active, suggesting that these fractions may also contain active GPR35 agonists.

Examining the real-time DMR characteristics further confirmed the assessment based on similarity analysis. For *Paederia scandens* extracts there are three clusters of fractions that were active in HT29 (**Supplementary Fig.S5**). The peak response was observed for JST-009 among the group of JST-007 to 010, JST-062 among the group of JST-061 to 065, and JST-067 among the group of JST-065 to JST-072. Furthermore, similar to JST-067, JST-009 greatly desensitized the DMR of YE210, suggesting that both contain a GPR35 agonist. However, JST-062 gave rise to a DMR distinct from YE210, and had little effect on the DMR of YE210, suggesting that JST-062 contains compound(s) that modulate cellular protein(s) distinct from GPR35. Literature mining showed that *Paederia scandens* extracts contain high amount of quercetin,[33] a known GPR35 partial agonist[40,43].

However, fractions of the *Millettia pachyloba* extracts gave rise to complicated pharmacological profiles in HT29 (**Supplementary Fig. S1 to S4**). The clear peak response was observed for DYT-007 in the group of DYT-006 to 009, DYT-081 in the group of DYT-080 to 084, DYT-085 in the group of DYT-085 to 090, DYT-098 in the group of DYT-096 to 099, DYT-106 in the group of DYT-104 to 107. For others, no clear isolated cluster can be identified. Furthermore, DYT-081, DYT-085, and DYT-097 triggered a DMR distinct from YE210, but greatly desensitized the YE210 DMR, suggesting that these fractions contain a GPR35 agonist, as well as compound(s) that modulate a different target. However, other fractions triggered a DMR similar to YE210, and desensitized the YE210 DMR to different degrees. Nonetheless, these results suggest that both plant extracts contain multiple GPR35 agonists, the exact of which are currently under investigation.

Identification of active compounds in JST-003 fraction

Next, we focused on the identification of active compound(s) in JST-003 using several approaches, given that the *Paederia scandens* extract displayed relatively clean agonist profiles in the three cell lines tested and JST-003 gave rise to the greatest DMR in A431 among the fraction group JST-001 to 004.

First, we compared the LC-MS profiles of the fraction group of JST-001 to 004. Both UV absorbance and MS (total ion chromatography with positive electrospray ionization mode, ESI+) were monitored. Results showed that there are markedly overlap in UV absorbance and total ion chromatograms among these fractions, although each crude fraction is a complex mixture (**Fig.4**). Based on the relative DMR signal amplitudes observed in A431, the peak around 2.65 most likely contains the active compound.

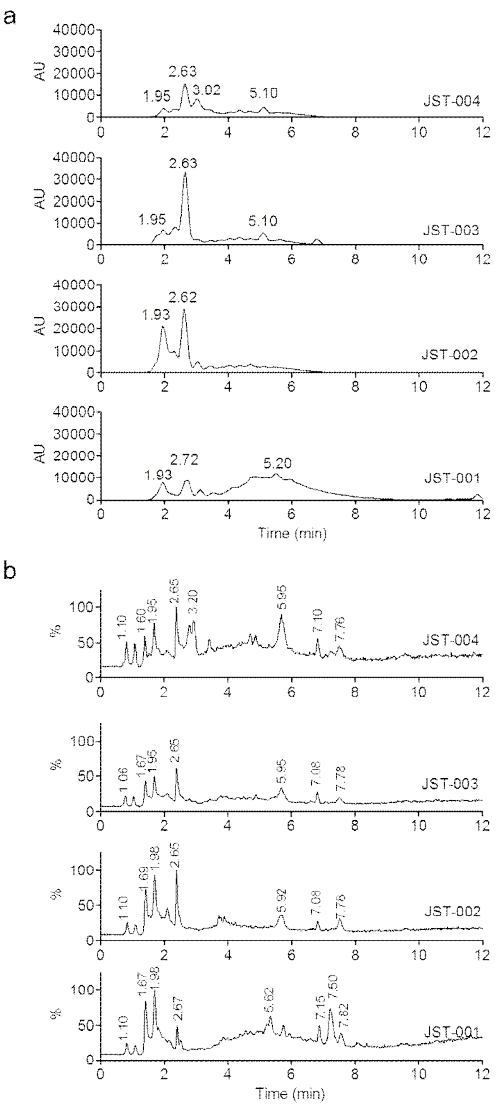

FIGURE 4. LC-MS analysis of the fraction group of JST-001 to 004. (a) UV chromatograms at 260nm. (b) Total ion MS chromatograms at positive ESI mode. Mobile phase A is 0.1% (v) formic acid in water and B is 0.1% (v) formic acid in acetonitrile. The gradient of separations was 0 min (5%, phase B)-15 min (95%, phase B). The flow rate was 1 ml/min.

Second, we increased the separation power of HPLC to prepare five secondary fractions from JST-003 based on both UV at 254nm and total ion chromatograms; these secondary fractions were named JST-003-#1 to JST-003-#5, corresponding to the peaks at 9.13, 12.48, 15.83, 19.78 and 24.32 min (**Fig.5a**). We then tested the dose responses of all five secondary fractions and found that only JST-003-#1 trigged a DMR similar to that observed in the initial screen, and

gave rise to a clear dose response with an apparent logEC_{50} in ng/ml of 2.78±0.03 (n=3) (**Fig.5b and c**). The relatively potency obtained suggests that this secondary fraction is also impure (see below).

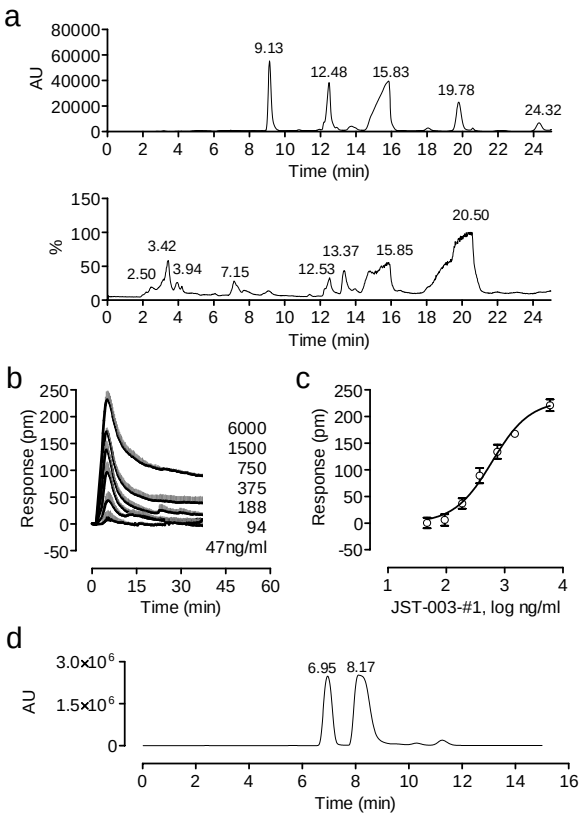

FIGURE 5. Analysis of the fraction JST-003. (a) UV (260nm, top) and total ion (positive ESI mode, bottom) MS chromatograms of JST-003. Mobile phase A is 0.1% (v) formic acid in water and B is 0.1% (v) formic acid in methanol. The gradient of separations was 0 min (3%, phase B)-15 min (25%, phase B)-20min (95%, phase B). The flow rate was 1 ml/min. The ten secondary fractions were collected as indicated by grey boxes. (b) Real-time dose response of JST-003-#1 in A431; (c) The maximal DMR amplitudes as a function of JST-003-#1 dose. Data represents mean ± s.d. (n=4). (d) Reverse phase isocratic HPLC purification of C1 and C2 from JST-003-#1 under UV chromatograms at 260nm. 0.1% (v) formic acid in water was used as mobile phase during 15 minutes separation. The flow rate was 1 ml/min.

Third, we scaled up the preparation of JST-003-#1. This fraction was collected based on the MS peak at 9.13 min (**Fig.5a**). This fraction was further separated on a second dimension orthogonal purification under reverse phase mode, wherein the XAqua column was used with a flow rate of 1 ml/min, and 0.1% (v) formic acid in water as the mobile phase lasting for 15 minutes. Results showed that this peak was separated to two peaks (6.95min and 8.17min), based on UV absorbance at 260nm. The two purified compounds were named **C1**, and **C2**, respectively. DMR agonist assay showed that only **C2** behaved similarly to the secondary fraction JST-003-#1, while **C1** was inactive in A431.

Fourth, we characterized **C2** using MS and NMR. MS showed that **C2** has an m/z of 123.97, and gave rise to a fragmented mass distribution pattern almost identical to niacin under high duty cycle mode with 180 voltages, leading to m/z of 106.0287 (-H2O), 96.0444 (-CO), 80.0495 (-CO2) and 78.0338 (-HCOOH) (**Supplementary Fig.6**). ^{1}H- and ^{13}C-NMR spectra of **C2** further confirmed that **C2** is niacin (^{1}H-NMR in D_2O: δ 7.978 (s, 1H), 8.783 (s, 2H), 9.052 (s, 1H); ^{13}C-NMR in D_2O: 126.801, 134.989, 142.849, 143.370, 145.354 and 169.663) (**Supplementary Fig.7**). Both NMR and MS results indicate that **C2** has a purity >98%.

Fifth, given that niacin was found to be the active component of JST-003-#1, we used selected ion m/z of 124 as the targeted species to re-examine the distribution of niacin within the fraction groups JST-001 to JST-004, and DYT-001 to DYT005. LC-MS analysis showed that the targeted molecule in these fractions is enriched in JST-003 with the peak at 2.38min (**Fig.6**), or DYT-003 with the peak at 2.65min (**Supplementary Fig.S8**), consistent with the DMR profiling results shown in **Fig.3**.

Together, these results showed that the chemical constituent in both herb extracts being active in A431 is niacin.

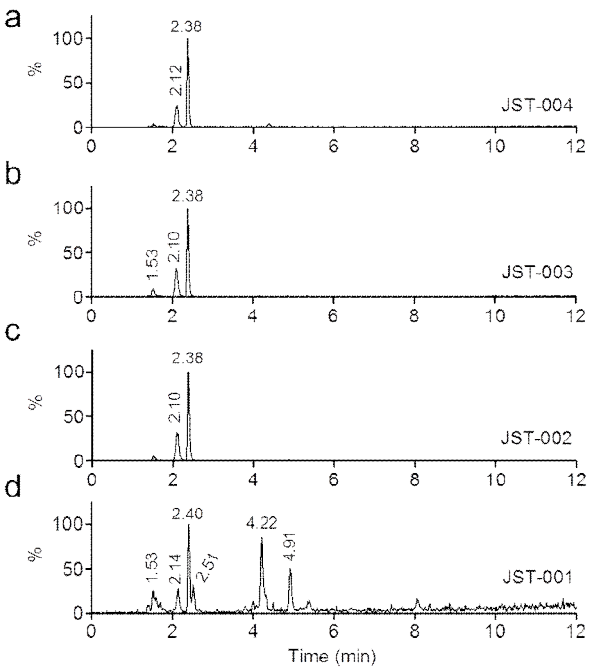

FIGURE 6. LC-MS analysis of the fraction group of JST-001 to 004 using selected ion chromatography with a targeted m/z of 124 at positive ESI mode. Mobile phase A is 0.1% (v) formic acid in water and B is 0.1% (v) formic acid in acetonitrile. The gradient of separations was 0 min (5%, phase B)-15 min (95%, phase B). The flow rate was 1 ml/min.

Characterization of hydroxyl carboxylic acid receptor-2 (HCA-2) in A431

Given that niacin is a known agonist for HCA2 and **C2** was found to trigger a rapid and transit DMR in A431, we hypothesized that the DMR of **C2** in A431 is due to the activation of endogenous HCA2 receptor. We employed several approaches including mRNA expression, DMR and cAMP assays to ascertain this hypothesis.

First, we performed quantitative RT-PCR of three receptors, HCA2, HCA3 and GPR35 in the three cell lines. HCA2 is a high affinity receptor for niacin, while HCA3 is a low affinity receptor for niacin.[46] Results showed that compared to the two control genes (ACTB, β-actin; HPRT1, hypoxanthine phosphoribosyltransferase 1), A431 expresses mRNAs for HCA2 and HCA3 both at high level, but little GPR35, while A549 expresses three receptors all at low level. In contrast, HT29 expresses mRNAs for GPR35 at high level, but HCA2 and HCA3 at moderate level.

Table 1 mRNA expression of different genes in three cell lines. The number is the cycle threshold value. For control genes, the numbers are mean ± s.d. (n=4)

Symbol	A431	A549	HT29
HCA2	20.02	28.96	26.04
HCA3	21.08	32.13	26.35
GPR35	33.49	28.88	22.43
HPRT1	21.01±0.21	21.05±0.30	22.04±0.35
ACTB	17.75±0.25	16.49±0.21	17.40±0.21

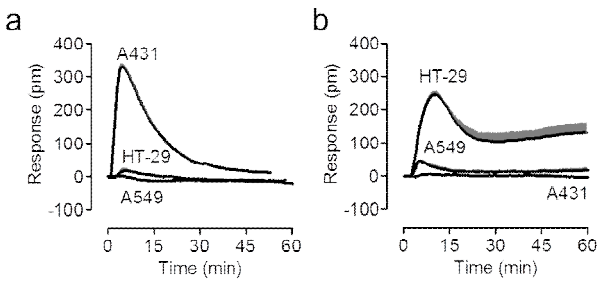

FIGURE 7. The DMR signals of 10μM niacin (a) and 10μM zaprinast (b) in A431, A549 and HT-29. Data represents mean ± s.d. (n=4).

Second, we profiled the endogenous receptors using known agonists. Consistent with receptor expression pattern, niacin at 10μM was found to trigger a robust DMR in A431, but led to very small DMR in HT29 and little DMR in A549 (**Fig.7a**). On the other hand, the know GPR35 full agonist zaprinast[45] triggered a robust DMR in HT29, a small DMR in A549, but little DMR in A431 (**Fig.7b**). The zaprinast DMR in the three cell lines further indicate that the second cluster including DYT-085 shown in **Fig.2** may contain GPR35 full agonists, given that except for JST-062 and 063, these fractions generally triggered a robust DMR in HT29, and a small DMR in A549, but little DMR in A431, a trend almost identical to zaprinast. However, the inability to detect any DMR in A459, a cell line endogenously expressing HCA2 and HCA3 mRNA at moderate level may be due to the relatively low protein level or signaling capacity of these receptors in this cell line, or the sensitivity of DMR assays that is still not high enough.

Third, we compared the DMR pharmacology of niacin and the purified **C2** in A431. DMR agonist assays showed that niacin and **C2** triggered identical dose responses, leading to indistinguishable $logEC_{50}$ of -7.39±0.02 and -7.46±0.03 (n=4), respectively (**Fig.8a** and **b**). Given the high potency observed, we concluded that the DMR of niacin is mostly originated from the activation of HCA2. Further, based on the potency of purified niacin obtained we estimated that the concentration of niacin in the JST-003-#1 fraction was 0.83%.

Fourth, we compared the pharmacology of niacin with its isomer isonicotinic acid, and two other known HCA2 agonists, nicofuranose and acipimox to further confirm the presence of functional HCA2 receptor in A431. Results showed that isonicotinic acid triggered a dose-dependent response, but with much smaller maximal amplitude and lower potency with a $logEC_{50}$ of -5.32±0.10 (n=4) than niacin (**Fig.8c and d**). On the other hand, the HCA2 full agonists nicofuranose and acipimox both gave rise to a maximal amplitude comparable to niacin; however, displayed distinct potency with $logEC_{50}$ of -6.60±0.04 and -5.99±0.01 (n=4), respectively (**Fig.8d**). As a negative control, nicotinly alcohol was found to be inactive in A431 (**Fig.8d**). These results further confirmed that A431 endogenously expresses functional HCA2 receptor.

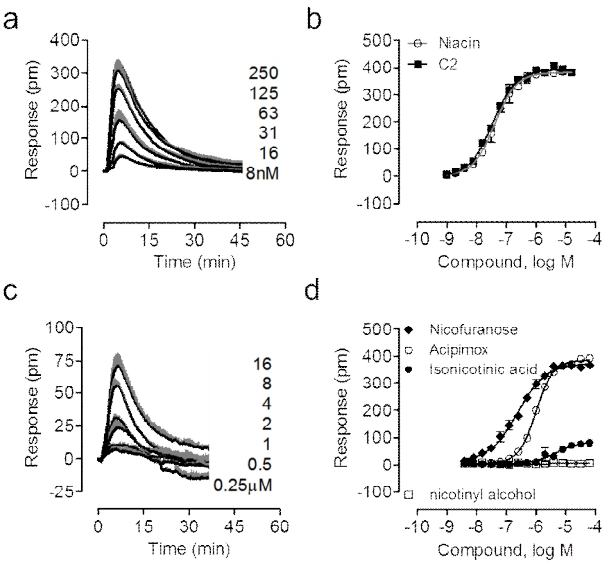

FIGURE 8. DMR dose responses of compounds in A431. (a,c) Real-time DMR of niacin (a) and isonicotinic acid (c). (b,d) DMR maximal amplitudes as a function of compound doses: niacin and C2 (b), nicofuranose, acipimox, isonicotinic acid and nicotinyl alcohol (d). Data represents mean ± s.d. (n=4).

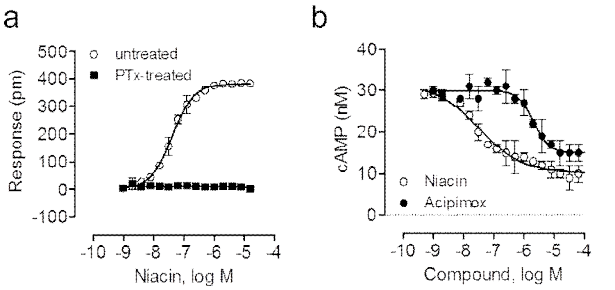

FIGURE 9. The dose responses of niacin in A431. (a) Dose DMR responses of niacin in untreated and PTx-treated A431 cells. The maximal DMR amplitudes were plotted as a function of niacin. (b) Dose inhibition of the cAMP signal induced by 5μM forskolin. Data represents mean±s.d from 2 independent measurements (n=4).

Fifth, we examined the ability of different ligands to desensitize the DMR arising from the subsequent stimulation with 1 μM niacin. Results showed that niacin, **C2**, nicofuranose and acipimox also dose-dependently desensitized the DMR of 1μM niacin, leading to an apparent of $logIC_{50}$ of -6.95±0.03, -7.14±0.05, -6.30±0.05, and -5.66±0.05 (n=4), respectively. In contrast, nicotinyl alcohol and isonicotinic acid were inactive. These results suggest that **C2** is indeed niacin, and nicofuranose and acipimox are strong partial agonists for HCA2, while nicotinyl alcohol is inactive at HCA2 or HCA3. However, the weak agonist activity of isonicotinic acid observed might act at the HCA3 or another unknown receptor expressed in A431; such a possibility is worthy further investigation.

Lastly, we deconvoluted the pathways responsible for the DMR of niacin using DMR pathway deconvolution assay.[44] Results showed that the pretreatment of A431 cells with PTx completely suppressed the dose response of niacin, suggesting that the niacin DMR is solely originated from the $G_{\alpha i}$ pathway (**Fig.9a**). PTx is known to result in the permanent inhibition of $G_{\alpha i}$ by ADP ribosylation of a cysteine of the protein.[47] cAMP assays showed that niacin itself did not cause cAMP accumulation, but dose-dependently suppressed the cAMP signal arising from the activation of adenylate cyclases by its known activator forskolin, leading to an apparent $logIC_{50}$ of -7.48±0.15 (**Fig.9b**). Acipimox behaved similarly, yielding an apparent $logIC_{50}$ of -5.68±0.07 (**Fig.9b**). The potency of both agonists obtained was similar to those obtained using DMR agonist assays (**Fig.8**).

Together, these results suggest that the DMR of niacin is due to the activation of endogenous and $G_{\alpha i}$-coupled HCA2 receptor in A431.

Total amount of niacin in *Paederia scandens* and *Millettia pachyloba* extracts

Next, we determined the amount of niacin in the two plants. Results showed that the LC-MS/MS method allows for determining the concentration of niacin in a linear range from 0.1 to 100 μg/ml with a calibration equation of Y=849+2967X (R^2 0.9999). Furthermore, out of 1g *Paederia scandens* and *Millettia pachyloba* plants, we obtained 171.28 and 145.98 mg solid extracts, and 2.94 and 2.25 μg niacin in total, respectively. Hence, the concentration of niacin in extracts is 17.0 and 15.4 μg/g for *Paederia scandens* and *Millettia pachyloba*, respectively. Compared to the amount of niacin (within the range of 1 to 66 μg/g) reported in a wide variety of edible wild mushrooms and flowers[48], these results suggest that both plants contain moderately high amount of niacin.

Lastly, we mined the literature describing the clinical features of *Paederia scandens* extracts. Results showed that as a generally recognized as safe TCM, *Paederia scandens* extracts have been used to treat uric acid nephropathy,[49] toothache, chest pain, piles, inflammation of the spleen, rheumatic arthritis and bacillary dysentery.[50-52] In a recent study, Zhang *et al.* studied the effects of *Paederia scandens* extracts on blood glucose and lipid in strepotozotocin-induced diabetic ICR mice (male with an average weight of 20±2.0g). They found that that once given by orally and daily for 30 days a high dose of the extracts (0.2ml 0.26g/ml extract solution) lowered the level of blood glucose by 7.6%, increased the level of cholesterol associated with ApoA-1/HDL particles, and lowered the triglycerides by 24.67%, suggesting that these extracts have a hypoglycemic effect.[53] The extract dose used was estimated to contain 0.90μg niacin, considering the concentration of niacin in the extract solid as we determined. Given that the total blood volume for 15-20g mice is about 0.8 to 1.75ml, the niacin concentration in mice blood could be as high as 9.1 to 4.2 μM, respectively. Another clinical study showed that the *Paederia scandens* extracts had markedly antihyperlipidemic beneficial effects on about 93% of patients with hyperlipidemia.[54] As the vitamin of the B complex niacin has been known to be the most effective lipid-lowering drug for over fifty years.[55,56] The β-arrestin mediated signaling via HCA2 receptor had been linked to the side effect, skin flushing, of niacin.[57] Niacin is thought to lower triglyceride levels by reducing hepatic VLDL synthesis through the activation of HCA2 receptor.[58-60] Although it still remains to be controversial whether the agonist activity of niacin at the HCA2 receptor is related to its antihyperlipidemic effect,[60] the moderately high amount of niacin in *Paederia scandens* extract obtained may be the underlined mechanism responsible for its anti-hyperlipidemic effect.

Conclusions

In the present paper we have presented a label-free cell phenotypic profiling-centric strategy to identify active chemical constituents of two TCM plants including *Paederia scandens* and *Millettia pachyloba*, and to determine their mechanisms of action. We found that both plant extracts contain moderately high amount of niacin. The presence of niacin in *Paederia scandens* extract may be linked to its anti-hyperlipidemic effect observed in diabetic mice and clinical setting. This study highlights the power of label-free cell phenotypic profiling for relating the active chemical constituents of medicinal plants to their clinical benefits and/or side effects, in general for drug discovery[62,63].

Acknowledgements

The authors gratefully acknowledge the financial support from Pillar Program of the 11th five-year Plan by China National Science & Technology (2008BAI51B01) and the project from China Natural Science Foundation (81274077).

Notes and references

[a] Key Laboratory of Separation Science for Analytical Chemistry, Dalian Institute of Chemical Physics, Chinese Academy of Sciences, Dalian, Liaoning 116023, China

[b] Biochemical Technologies, Science and Technology Division, Corning Incorporated, Corning, New York 14831, United States of America.

‡ These authors contributed equally to this work.

* E-mail: liangxm@dicp.ac.cn (X.L.); fangy2@corning.com (Y.F.).

† Electronic Supplementary Information (ESI) available: Supplementary Figure S1-5 shows the DMR signal of active fractions in HT29 cells, and the DMR of YE210 after the pretreatment with active fractions. Supplementary Figure S6 shows mass spectra of **C2**. Supplementary Figure S7 shows NMR spectra of **C2**. Supplementary Figure S8 shows LC-MS spectra with a targeted m/z of 124 of the fraction group of DYT-001 to 005. See DOI: 10.1039/b000000x/

1 B.M. Schmidt, D.M. Ribnicky, P.E. Lipsky, L. Raskin, *Nat. Chem. Biol.* 2007, **3**, 360–366.
2 T.W. Corson, C.M. Crews, *Cell* 2007, **130**, 769–774.
3 D.X. Kong, X.J. Li, G.Y. Tang, H.Y. Zhang, *ChemMedChem* 2008, **3**, 233–236.
4 L. Zhou, Z. Zuo, M.S. Chow, *J. Clin. Pharmacol*. 2005, **45**, 1345-1359.
5 Y. Chu, L. Zhang, X.Y. Wang. J.H. Guo, Z.X. Guo, X.H. Ma, *J. Ethnopharmacol.* 2011, **137**, 1457–1461.
6 F.E. Koehn, G.T. Carter, *Nat. Rev. Drug Discov.* 2005, **4**, 206–220.
7 D.D. Baker, M. Chu, U. Oza, V. Rajgarhia, *Nat. Prod. Rep*. 2007, **24**, 1225–1244.
8 D.-X. Kong, X.-J. Li, H.-Y. Zhang, *ChemMedChem* 2008, **3**, 1169–1171.
9 P. Hunter, *EMBO Rep*. 2008, **9**, 838–840.
10 M.C. Desai, S. Chackalamannil, *Curr. Opin. Drug Discov. Devel.* 2008, **11**, 436–437.
11 D.J. Newman, *J. Med. Chem*. 2008, **51**, 2589–2599.
12 A.L. Harvey, *Drug Discov. Today* 2008, **13**, 894–901.
13 J.W. Li, J.C. Vederas, *Science* 2009, **325**, 161-165.
14 M.J. Balunas, A.D. Kinghorn, *Life Sci.* 2005, **78**, 431-441.
15 D.J. Newman, G.M. Cragg, *J. Nat. Prod.* 2012, **75**, 311-335.
16 F. Zhu, X.H. Ma, C. Qin, L. Tao, X. Liu, Z. Shi, C.L. Zhang, C.Y. Tan, Y.Z. Chen, Y. Jiang, *PLoS ONE* 2012, **7**, e39782.
17 W. Weber, M. Fussenegger, *Drug Discov. Today* 2009, **14**, 956-963.
18 D.C. Swinney, J. Anthony, *Nat. Rev. Drug Discov*. 2011, **10**, 507-519.
19 E. Tran, Y. Fang, *J. Biomol. Screen.* 2008, **13**, 975-985.
20 K. Dodgson, L. Gedge, D.C. Murray, M. Coldwell, *J. Recept. Signal Transduct. Res*. 2009, **29**, 163-172.
21 Y. Fang, *Expert Opin. Drug Discov*. 2011, **6**, 1285-1298.
22 Y. Fang, A.M. Ferrie, N.H. Fontaine, J. Mauro, J. Balakrishnan, *Biophys. J*. 2006, **91**, 1925-1940.
23 Y. Fang, A.M. Ferrie, N.H. Fontaine, P.K. Yuen, *Anal. Chem*. 2005, **77**, 5720-5725.
24 F. Verrier, S. An, A.M. Ferrie, H. Sun, M. Kyoung, Y. Fang, S.J. Benkovic, *Nat. Chem. Biol.* 2011, **7**, 909–915.
25 R. Schröder, N. Janssen, J. Schmidt, A. Kebig, N. Merten, S. Hennen, A. Müller, S. Blättermann, M. Mohr-Andrä, S. Zahn, J. Wenzel, N.J. Smith, J. Gomeza, C. Drewke, G. Milligan, K. Mohr, E. Kostenis, *Nat. Biotech*. 2010, **28**, 943–949.
26 A.M. Ferrie, H. Sun, Y. Fang, *Sci. Rep*. 2011, **1**, 33.
27 H. Deng, C. Wang, M. Su, Y. Fang, *Anal. Chem*. 2012, **84**, 8232−8239.
28 R. Schrage, W.K. Seemann, J. Klöckner, C. Dallanoce, K. Racké, E. Kostenis, M. De Amici, U. Holzgrabe, K. Mohr, *Br. J. Pharmacol.* 2013, **169**, 357-370.
29 C. Chu, Y. Huang, Y.-F. Chen, J.-H. Wu, K. Rahman, H.-C. Zheng, L.-P. Qin, *J. Ethnopharmacol*. 2008, **118**, 177-180.
30 N.Q. Dang, H. Toshihiro, T. Masami, X.D. Nguyen, A. Yoshinori, *Phytochemistry* 2002, **60**, 505–514.
31 Y.L. Kim, Y.W. Chin, J. Kim, J.H. Park, *Chem. Pharm. Bull*. 2004, **52**, 1356–1357.
32 J-L. Xu, L. Liu, Q.-Y. Zhang, L.-P. Qin, *J. Pharmaceutical Practice (Chinese)* 2011, **29**, 402-404.
33 N. Ishikura, Z.Q. Yang, K. Yoshitama, K. Kurosawa, *Z. F. Naturforsch. J. Biosci.* 1990, **45**, 1081-1084.
34 G. Li, A.M. Ferrie, Y. Fang, *J. Assoc. Lab. Autom*. 2006, **11**, 181-187.
35 Y. Fang, *Sensors* 2007, **7**, 2316-2329.
36 M. Morse, E. Tran, R.L. Levension, Y. Fang, *PLoS One* 2011, **6**, e25643.
37 M. Morse, H. Sun, E. Tran, R. Levenson, Y. Fang, *BMC Pharmacol. Tox*. 2013, **14**, 17.
38 K.E. Heim, A.R. Tagliaferro, D.J. Bobilya, *J. Nutr. Biochem*. 2002, **13**, 572-584.
39 F. Ververidis, E. Trantas, C. Douglas, G. Vollmer, G. Kretzschmar, N. Panopoulos, *Biotechnol. J.* 2007, **2**, 1214-1234.
40 L. Jenkins, J. Brea, N.J. Smith, B.D. Hudson, G. Reilly, N.J. Bryant, M. Castro, M.I. Loza, G. Milligan, *Biochem. J.* 2010, **432**, 451−459.
41 H. Deng, Y. Fang, *Pharmacology* 2012, **89**, 211-219.
42 H. Deng, Y. Fang, *Pharmaceuticals* 2013, **6**, 500-509.
43 H. Deng, H. Hu, S. Ling, A.M. Ferrie, Y. Fang, *ACS Med. Chem. Lett.* 2012, **3**, 165–169.
44 A.M. Ferrie, C. Wang, H. Deng, Y. Fang, *Integr. Biol.* 2013, **5**, 1253-1261.
45 H. Deng, H. Hu, M. He, J. Hu, W. Niu, A.M. Ferrie, Y. Fang, *J. Med. Chem*. 2011, **54**, 7385–7396.
46 S. Offermanns, S.L. Colletti, T.W. Lovenberg, G. Semple, A. Wise, A.P. IJzerman, *Pharmacol. Rev.* 2011, **63**, 269-290.
47 H. Deng, H. Sun, Y. Fang, *J. Pharmacol. Tox. Methods* 2013, **68**, 323–333.
48 H. Wang, Y. Chen, L. Zhou, *Food Sci.* (Chinese) 2000, **21**, 53-54.
49 Y.F. Chen, Y. Huang, W.Z. Tang, L.P. Qin, H.C. Zheng, *Pharmacol. Biochem. Behav*. 2009, **93**, 97-104.
50 J. Choi, K.T. Lee, M.Y. Choi, J.H. Nam, H.J. Jung, S.K. Park, H.J. Park, *Biol. Pharmaceut. Bull*. 2005, **28**, 1915–1918.
51 W. Jiang, D. Jin, Z. Li, Z. Sun, M. Chen, B. Wu, C. Huang, *Biomed. Chromatogr*. 2012, **26**, 863-868.
52 Y.F. Chen, J.Y. Zhang, M.H. Zhao, M. Yan, Q.C. Zhao, Q. Wu, H. Jin, G.B. Shi, *Pharmacol. Biochem. Behav*. 2012, **102**, 585-592.
53 X.F. Zhang, B.P. Ji, H.J. Zhang, B. Li, H.Q. Yu, *Food Sci.* (Chinese) 2008, **29**, 282-295.
54 Y.L. Dai, *Yunnan Zhongyi Zhongyao Zazhi* (Chinese) 2005, **26**, 20-21.
55 R.H. Knopp, *N. Engl. J. Med*. 1999, **341**, 498-511.

56 S. Tunaru, J. Kero, A. Schaub, C. Wufka, A. Blaukat, K. Pfeffer, S. Offermanns, *Nat. Med*. 2003, **9**, 352-355.
57 R.W. Walters, A.K. Shukla, J.J. Kovacs, J.D. Violin, S.M. DeWire, C.M. Lam, J.R. Chen, M.J. Muehlbauer, E.J. Whalen, R.J. Lefkowitz, *J. Clin. Invest.* 2009, **119**, 1312-1321.
58 J.E. Digby, J.M. Lee, R.P. Choudhury, *Curr. Opin. Lipidol.* 2009, **20**, 321–326.
59 J.C. Creider, R.A. Hegele, T.R. Joy, *Nat. Rev. Endocrinol.* 2012, **8**, 517-528.
60 E.T. Bodor, S. Offermanns, *Br. J. Pharmacol.* 2008, **153** Suppl 1: S68-S75.
61 B. Lauring, A.K. Taggart, J.R. Tata, R. Dunbar, L. Caro, K. Cheng, J. Chin, S.L. Colletti, J. Cote, S. Khalilieh, J. Liu, W.L. Luo, A.A. Maclean, L.B. Peterson, A.B. Polis, W. Sirah, T.J. Wu, X. Liu, L. Jin, K. Wu, P.D. Boatman, G. Semple, D.P. Behan, D.T. Connolly, E. Lai, J.A. Wagner, S.D. Wright, C. Cuffie, Y.B. Mitchel, D.J. Rader, J.F. Paolini, M.G. Waters, A. Plump, *Sci. Transl. Med.* 2012, **4**, 148ra115.
62 Y. Fang, *J. Pharmacol. Tox. Methods* 2013, **67**, 69-81.
63 Y. Fang, *Front.Pharmacol.* 2014, **5**, 52.

For TOC only

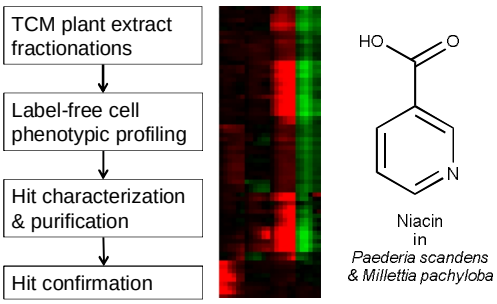

Label-free cell phenotypic profiling with three cell lines identified multiple pharmacologically active compounds including niacin in two TCM plants.

